ESTIMATES- AND CORRECTOR-BASED MESH ADAPTATION

GAUTIER BRÈTHES[1], ADRIEN LOSEILLE[2], FRÉDÉRIC ALAUZET[3] AND ALAIN DERVIEUX[4]

[1]INRIA
2004 Route des lucioles, F-06902 Sophia Antipolis
Gautier.Brethes@inria.fr
http://www-sop.inria.fr/members/Gautier.Brethes/Gautier.Brethes.htm

[2]INRIA
BP 105, Domaine de Voluceau, F-78153 Le Chesnay
Adrien.Loseille@inria.fr
https://www-roc.inria.fr/gamma/gamma/Membres/CIPD/Adrien.Loseille/index.php

[3]INRIA
BP 105, Domaine de Voluceau, F-78153 Le Chesnay
Frederic.Alauzet@inria.fr
https://www-roc.inria.fr/gamma/gamma/Membres/CIPD/Frederic.Alauzet/index.en.html

[4]INRIA
2004 Route des lucioles, F-06902 Sophia Antipolis
Alain.Dervieux@inria.fr
http://www-sop.inria.fr/members/Alain.Dervieux/Alain_Dervieux-french.html

Key words: Poisson problem, Compressible flow, goal-oriented mesh adaptation, anisotropic mesh adaptation, adjoint, metric

Abstract. We present a novel formulation for the mesh adaptation of the approximation of a PDE. The proposed formulation extends the goal-oriented formulation, since it is equation-based and uses an adjoint. At the same time, it supersedes it as a solution-convergent method. Indeed, goal-oriented methods rely on the reduction of the error in evaluating a chosen scalar output with the consequence that as mesh size is increased (more degrees of freedom) only this output is proven to tend to its continuous analog, while the solution field itself may not converge. A remarkable throughput of goal-oriented metric-based adaptation is the mathematical formulation of the mesh adaptation problem under the form of the optimization, in the well-identified set of metrics, of a well-defined functional. In the new proposed formulation, we amplify this advantage. We search, in the same well-identified set of metrics, the minimum of a norm of the approximation error. The norm is prescribed by the user and the method allows addressing the case of multi-objective adaptation, like, for example in aerodynamics, adapting the mesh for drag, lift,

1

moment in one shot. In this work we consider the basic linear finite-element approximation and restrict our study to L^2 norm in order to enjoy second-order convergence. Numerical examples for the 2D Poisson problem and for 3D Euler flows are computed.

1 INTRODUCTION

Most simulation processes start with a smart Partial Differential Equation (PDE) and finish with a step of discretisation and approximate solution. The deviation between the continuous PDE solution and its approximation on a mesh is one of the most imperfect step of the simulation since the mesh is not chosen on completely rigorous bases. Now the engineer knows well what he/she expects: typically an approximation error sufficiently smaller than some level (frequently dimensioned by the model error). The approximation step is rather well specified: find the mesh for the given error level. Therefore, finding the best mesh would simply be a minimisation problem (looking for the mesh of specified total size, which makes the error minimum). However, a mesh does not lie in a suitable space for minimisation: a mesh is a combination of coordinates and of a kind of graph. Thus going towards the discrete world is a simplification for the unknown field, and an enormous complexification in finding a new unknown, the mesh. With the arising of Hessian-based mesh adaptation methods, e.g. [6, 5], it appeared that an anisotropic mesh can be parameterized by a continuous field defined on the computational domain, the metric. The idea of continuous metric or continuous mesh has been further formalised in [9, 10]. It remains to decide which error functional will be minimised with respect to the metric. Again, this functional should be continuous.

In Hessian-based method, the P1-interpolation error is transformed in terms of a product of continuous Hessian by ingredients from the metric (see [14] for details). The optimal continuous metric is then uniquely defined in terms of the Hessian, via the continuous metric optimality conditions. Only at the end of the process, these optimality conditions are discretised to produce an approximate optimal metric. This approach has permitted powerful anisotropic unstructured mesh adaptations.

Hessian-based method do not take into account the PDE. Consequently, it can miss important features in the solution, in particular for advective dominated PDE. In contrast, goal-oriented formulations consider a scalar output error which is expressed in terms of the approximation global error. The approximation global error is essentially solution of the linearised PDE with a local error as RHS. This results in the use of an adjoint state. In [8], the minimisation problem is expressed in terms of interpolation errors weighted by functions of the adjoint. Again, the minimum of the continuous scalar output error is uniquely defined. Again, the continuous optimality system is at last discretised.

In the new norm-oriented formulation proposed in this paper, the user can prescribe a norm or a semi-norm $|u - u_h|$ of the error, in order to minimise it with respect to the mesh. As a typical example of semi-norm, this can be the sum of square deviations on

particular outputs. Let us take an example in aerodynamics. The semi-norm $|u - u_h| \equiv |C_l(u) - C_l(u_h)|^2 + |C_d(u) - C_d(u_h)|^2 + |C_m(u) - C_m(u_h)|^2$ will account for minimising the errors on lift, drag, moment measured from flow solution u_h with respect to the mesh. The proposed method will ultimately address this kind of semi-norm, assuming that, as for the goal-oriented method, the issue of a non-admissible norm is solved. As for the goal-oriented method, the proposed method takes into account the PDE features and, in case where a norm is prescribed, it produces an approximate solution field which does converge to the exact one in this norm. In this paper, the method is first demonstrated with the usual linear finite-element method in 2D. This approximation is first-order accurate for H^1 norm, but second-order accurate for L^2 norm, which we shall consider here. The method relies on the use of a corrector field, and on an *a priori* error estimate from which is extracted the asymptotically largest terms of the local error.

The derivation of a corrector is proposed in Sec. 2. Next two sections are devoted to the three identified mesh adaptation formulations: a Hessian-based, minimizing an interpolation error in Sec. 3, a goal-oriented formulation and our proposal for a norm-oriented in Sec. 4. Sec. 5 is devoted to a numerical comparison between the two field-convergent formulations, *viz.* Hessian-based and norm-oriented for an elliptic PDE. Sec. 6 addresses the Euler PDE of aerodynamics.

2 FINER-GRID CORRECTOR FOR A GENERIC PDE

We consider a linear PDE denoted $Au = f$ and a second-order accurate discretization of it, $A_h u_h = f_h$. Let us assume the problem is smooth and that the approximation is in its asymptotic mesh convergence phase for the mesh Ω_h under study, of size h. Then this will be also true for a strictly two-times finer embedding mesh $\Omega_{h/2}$. We would have:

$$u_h = A_h^{-1} f_h \quad , \quad u_{h/2} = A_{h/2}^{-1} f_{h/2} \quad \Rightarrow \quad u - u_{h/2} \approx \frac{1}{4}(u - u_h) \tag{1}$$

where u_h and $u_{h/2}$ are respectively the solutions on Ω_h and $\Omega_{h/2}$. We have also $\Pi_h u - \Pi_h u_{h/2} \approx \frac{1}{4}(\Pi_h u - u_h)$. This motivates the definition of a finer-grid Defect-Correction (DC) corrector as follows:

$$A_h \bar{u}'_{DC} = \frac{4}{3} R_{h/2 \to h}(A_{h/2} P_{h \to h/2} u_h - f_{h/2}) \tag{2}$$

where the residual transfer $R_{h/2 \to h}$ accumulates on coarse grid vertices the values at fine vertices in neighboring coarse elements multiplied with barycentric weights, and $P_{h \to h/2}$ linearly interpolates coarse values on fine mesh. In the case of local singularities, statement (1) is not true for uniform meshes, but we have some hints that it holds almost everywhere for a sequence of adapted meshes, according to [12]. The DC corrector $\bar{u}'_{DC}$ approximates $\Pi_h u - u_h$ instead of $u - u_h$ and can be corrected as the previous one:

$$u'_{DC} = \bar{u}'_{DC} - (\pi_h u_h - u_h). \tag{3}$$

This field will play a key role in the norm-oriented mesh adaptation introduced in the sequel.

3   INTERPOLATION ERROR OPTIMIZATION

3.1   Mesh parametrization

We propose to work in the continuous mesh framework, introduced in [9, 10]. The main idea of this framework is to model discrete meshes by continuous Riemannian metric fields. It allows us to define the adaptation problem as a differentiable optimization problem , *i.e.*, to apply on the class continuous metrics a calculus of variations which cannot be applied on the class of discrete meshes. This framework lies in the class of metric-based methods. A continuous mesh $\mathcal{M}$ of the computational domain Ω is identified to a Riemannian metric field [3] $\mathcal{M} = (\mathcal{M}(\mathbf{x}))_{\mathbf{x} \in \Omega}$ where $\mathcal{M}(\mathbf{x})$ is a symmetric 3×3 matrix. We define the *total number of vertices* of $\mathcal{M}$ as:

$$\mathcal{C}(\mathcal{M}) = \int_{\Omega} \sqrt{\det(\mathcal{M}(\mathbf{x}))} \, \mathrm{d}\mathbf{x}.$$

Given a continuous mesh $\mathcal{M}$, we shall say that a discrete mesh $\mathcal{H}$ of the same domain Ω is a *unit mesh with respect to* $\mathcal{M}$, if each triangle $K \in \mathcal{H}$, defined by its list of edges $(\mathbf{a}_i \mathbf{b}_i)_{i=1\dots3}$, verifies:

$$\forall i \in [1,3], \quad \int_0^1 \sqrt{{}^t\mathbf{a}_i\mathbf{b}_i \, \mathcal{M}(\mathbf{a}_i + t \, \mathbf{a}_i\mathbf{b}_i) \, \mathbf{a}_i\mathbf{b}_i} \, \mathrm{d}t \in \left[\frac{1}{\sqrt{2}}, \sqrt{2} \right] .$$

The rest of the paper will try to find the best metric $\mathcal{M}$ from various error analyses.

3.2   Interpolation-based optimal metric

Let u be any smooth enough function defined on Ω. Let $\mathcal{M}$ be a mesh/metric of Ω. We consider only meshes $\mathcal{M}$ involving enough nodes for justifying the replacement of the complete error by its main asymptotic part. The P^1 interpolation error $|\Pi_{\mathcal{M}}u - u|$ can be approximated in terms of second derivatives of u and of the metric $\mathcal{M}$ by the *continuous interpolation error:*

$$|\Pi_{\mathcal{M}}u - u| \approx |u - \pi_{\mathcal{M}}u| \text{ with } |u - \pi_{\mathcal{M}}u|(\mathbf{x}) \quad = \quad \frac{1}{10}\mathrm{trace}(\mathcal{M}^{-\frac{1}{2}}(\mathbf{x}) \, |H_u(\mathbf{x})| \, \mathcal{M}^{-\frac{1}{2}}(\mathbf{x})) \,(4)$$

where $|H_u|$ is deduced from H_u by taking the absolute values of its eigenvalues. Starting from:

$$\|u - \pi_{\mathcal{M}}u\|_{\mathbf{L}^p(\Omega_h)} = \left(\int_{\Omega} \left(\mathrm{trace}\big(\mathcal{M}^{-\frac{1}{2}}(\mathbf{x})|H_u(\mathbf{x})|\mathcal{M}^{-\frac{1}{2}}(\mathbf{x})\big) \right)^p \mathrm{d}\mathbf{x} \right)^{\frac{1}{p}} \qquad (5)$$

we define as optimal metric the one which minimizes the right hand side under the constraint of a total number of vertices equal to a parameter N. After solving analytically

this optimization problem, we get the unique optimal $(\mathcal{M}_{\mathbf{L}^p}(\mathbf{x}))_{\mathbf{x}\in\Omega}$ as:

$$\mathcal{M}_{\mathbf{L}^p} = \mathcal{K}_p(H_u) = D_{\mathbf{L}^p}\left(\det|H_u|\right)^{\frac{-1}{2p+2}}|H_u| \ \text{ and } \ D_{\mathbf{L}^p} = N\left(\int_\Omega (\det|H_u|)^{\frac{p}{2p+2}}\right)^{-1}, \quad (6)$$

where $D_{\mathbf{L}^p}$ is a global normalization term set to obtain a continuous mesh with complexity N and $(\det|H_u|)^{\frac{-1}{2p+2}}$ is a local normalization term accounting for the sensitivity of the $\mathbf{L}^p$ norm. In the case of an adaptation loop for solving a Partial Differential Equation, a continuous function u is not available, only an approximate solution $u_\mathcal{M}$ is available. In that case, the continuous interpolation error (4) is replaced by:

$$|u_\mathcal{M} - \pi_\mathcal{M}u_\mathcal{M}|(\mathbf{x}) \ = \ \frac{1}{10}\text{trace}(\mathcal{M}^{-\frac{1}{2}}(\mathbf{x})\,|H_{u_\mathcal{M}}(\mathbf{x})|\,\mathcal{M}^{-\frac{1}{2}}(\mathbf{x})) \quad (7)$$

where $H_{u_\mathcal{M}}$ is an approximate Hessian evaluated with the patch-recovery approximation defined in [14]. According to the continuous mesh framework, statement (6) defines directly a continuous optimal metric. In practice, solving (6) is done by approximation, i.e. in a discrete context with a couple (mesh, solution) denoted $(\mathcal{H}_\mathcal{M}, u_\mathcal{M})$ and iteratively through the following fixed point:

Step 1: compute the discrete state $u_\mathcal{M}$ on mesh $\mathcal{H}_\mathcal{M}$,

Step 2: compute sensor $s_\mathcal{M} = s(u_\mathcal{M})$ and optimal metric $\mathcal{M}_{inter}^{opt} = \mathcal{K}_p(H_\mathcal{M}(s_\mathcal{M}))$,

Step 3: $\mathcal{M} = \mathcal{M}_{inter}^{opt}$, generate $\mathcal{H}_\mathcal{M} = \mathcal{H}_{\mathcal{M}_{inter}^{opt}}$ and go to 1, until convergence.

In our Hessian-based numerical examples, the L^2 case, $p = 2$, has been considered. The above notation $\mathcal{K}_p$ will also be used in the next sections for $p = 1$.

4 EQUATION-BASED ADAPTATION

4.1 Scalar output "goal-oriented" analysis

The goal-oriented analysis relies on the minimization of the error $\delta j_{goal}(\mathcal{M})$ committed on a scalar output $j = (g, u)$, error which we simplify as follows:

$$\delta j_{goal}(\mathcal{M}) = |(g, u - u_\mathcal{M})| = |(g, \Pi_\mathcal{M}u - u_\mathcal{M} + u - \Pi_\mathcal{M}u)|. \quad (8)$$

The term $u - \Pi_\mathcal{M}u$, similar to the main term of the Hessian-based adaptation in Section 3.2, can be explicitly approached in the same way. The term $\Pi_\mathcal{M}u - u_\mathcal{M}$ will be transformed via a discrete adjoint state $u_{g,\mathcal{M}}^*$ defined by:

$$\forall\psi \in \ V_\mathcal{M}, \quad a(\psi_\mathcal{M}, u_{g,\mathcal{M}}^*) = (\psi_\mathcal{M}, g). \quad (9)$$

Then:

$$\delta j_{goal}(\mathcal{M}) = |a(\Pi_\mathcal{M}u - u_\mathcal{M}, u_{g,\mathcal{M}}^*) + (g, u - \Pi_\mathcal{M}u)|$$

And introducing the continuous interpolation error (7):

$$\delta j_{goal}(\mathcal{M}) \preceq |a(\Pi_\mathcal{M}u - u_\mathcal{M}, u_{g,\mathcal{M}}^*)| + |g||\pi_\mathcal{M}u_\mathcal{M} - u_\mathcal{M}|$$

The first variational term can be estimated as in [1]:

$$\delta j_{goal}(\mathcal{M}) \preceq \int_{\Omega} \left(\, [\frac{1}{\rho}\bar{\rho}(H(u_{g,\mathcal{M}}^*)) + |g|] \, |\pi_{\mathcal{M}}u_{\mathcal{M}} - u_{\mathcal{M}}| \, + \, |u_{g,\mathcal{M}}^*| \, |\pi_{\mathcal{M}}f - f| \right) \, \mathrm{d}\Omega.$$

Where we have introduced the discrete extension of the interpolation error. It is then reasonable to try to minimize the RHS of this inequality instead of the LHS. But this involves still some difficulty due to the dependancy of adjoint state $u_{g,\mathcal{M}}^*$ with respect to $\mathcal{M}$. We shall further simplify our functional by freezing, during a part of the algorithm, the adjoint state. The idea is that, when we change the parameter $\mathcal{M}$, $u_{g,\mathcal{M}}^*$ is close to its (non-zero) continuous limit and is not much affected, in contrast to the interpolation errors $|\pi_{\mathcal{M}}u_{\mathcal{M}} - u_{\mathcal{M}}|$ and $|\pi_{\mathcal{M}}f - f|$. We then consider, for a given $\mathcal{M}_0$, the following optimum problem:

$$\min_{\mathcal{M}} \int_{\Omega} \left(\, [\frac{1}{\rho}\bar{\rho}(H(u_{g,\mathcal{M}_0}^*)) + |g|] \, |\pi_{\mathcal{M}}u_{\mathcal{M}} - u_{\mathcal{M}}| \, + \, |u_{g,\mathcal{M}_0}^*| \, |\pi_{\mathcal{M}}f - f| \right) \, \mathrm{d}\Omega.$$

This will produce an optimum:

$$\mathcal{M}_{opt,\mathcal{M}_0} = \arg\min_{\mathcal{M}} |tr(\mathcal{M}^{-1/2} \left([\frac{1}{\rho}\bar{\rho}H(u_{g,\mathcal{M}_0}^*) + |g|]|H_u| + |u_{g,\mathcal{M}_0}^*||H_f| \right) \mathcal{M}^{-1/2})|.$$

Observing that in the integrand

$$H_{goal,0} = [\frac{1}{\rho}\bar{\rho}(H(u_{g,\mathcal{M}_0}^*)) + |g|] \, |H_u| \, + \, |u_{g,\mathcal{M}_0}^*| \, |H_f|$$

is a positive symmetric matrix, we can apply the above calculus of variation and get:

$$\mathcal{M}_{opt,\mathcal{M}_0} = \mathcal{K}_1(\, [\frac{1}{\rho}\bar{\rho}(H(u_{g,\mathcal{M}_0}^*)) + |g|] \, |H_u| \, + \, |u_{g,\mathcal{M}_0}^*| \, |H_f|).$$

This solution can then be introduced in a fixed-point loop and will produce:

$$\mathcal{M}_{opt,goal} = \mathcal{K}_1(\, [\frac{1}{\rho}\bar{\rho}(H(u_{g,\mathcal{M}_{opt,goal}}^*)) + |g|] \, |H_u| \, + \, |u_{g,\mathcal{M}_{opt,goal}}^*| \, |H_f|).$$

Let us precise how the discrete algorithm is organised:
Step 1: compute the discrete state $u_{\mathcal{M}}$ on mesh $\mathcal{H}_{\mathcal{M}}$,
Step 2: compute the discrete adjoint state $W_{\mathcal{M}}^*$,
Step 3: compute optimal metric $\mathcal{M}_{opt,\mathcal{M}}$,
Step 4: $\mathcal{M} = \mathcal{M}_{opt,\mathcal{M}}$, generate $\mathcal{H}_{\mathcal{M}}$ and go to 1, until convergence.
  The adaptation of this process to the Euler model of Gas Dynamics is studied in [11] for the steady case and in [2] for the unsteady case.

4.2   Norm-based functional

We are now interested by the minimization of $\delta j(\mathcal{M}) = ||u - u_{\mathcal{M}}||^2_{L^2(\Omega)}$ with respect to the mesh $\mathcal{M}$. Introducing u'_{DC} from (3) gives:

$$\delta j(\mathcal{M}) \approx (u'_{DC}, u - u_{\mathcal{M}}). \tag{10}$$

Let us define the discrete adjoint state $u^*_{\mathcal{M}}$:

$$\forall \psi \in V_{\mathcal{M}}, \quad a(\psi_{\mathcal{M}}, u^*_{\mathcal{M}}) = (\psi_{\mathcal{M}}, u'_{DC}). \tag{11}$$

Then, similarly to Section 4.1, we have to solve the following optimum problem.

$$\min_{\mathcal{M}} \int_{\Omega} \left(\left[\frac{1}{\rho} \bar{\rho}(H(u^*_{\mathcal{M}})) + |u'_{DC}| \right] |\pi_{\mathcal{M}} u_{\mathcal{M}} - u_{\mathcal{M}}| + |u^*_{\mathcal{M}}| |\pi_{\mathcal{M}} f - f| \right) \, \mathrm{d}\Omega.$$

Exactly as for Section 4.1, we freeze the dependancy of the adjoint state.

$$\min_{\mathcal{M}} \int_{\Omega} \left(\left[\frac{1}{\rho} \bar{\rho}(H(u^*_{\mathcal{M}_0})) + |u'_{DC}| \right] |\pi_{\mathcal{M}} u_{\mathcal{M}} - u_{\mathcal{M}}| + |u^*_{\mathcal{M}_0}| |\pi_{\mathcal{M}} f - f| \right) \, \mathrm{d}\Omega.$$

$$\mathcal{M}_{opt,\mathcal{M}_0} = \mathcal{K}_1 \left(\left[\frac{1}{\rho} \bar{\rho}(H(u^*_{\mathcal{M}_0})) + |u'_{DC}| \right] |H_u| + |u^*_{\mathcal{M}_0}| |H_f| \right).$$

In order to get the final norm-oriented optimum $\mathcal{M}_{opt,norm}$ we shall:

Step 1: first solve the linearised corrector system (3) in order to get u'_{DC},

Step 2: then solve the adjoint system:

$$a(\psi, u^*_{DC,\mathcal{M}}) = (u'_{DC}, \psi) \tag{12}$$

Step 3: finally put:

$$\mathcal{M}^{(\alpha+1)} = \mathcal{K}_1 \left(\left[|u'_{DC}| + \frac{1}{\rho} \bar{\rho} H(u^*_{prio}) \right] |H_{u_{\mathcal{M}}}| + |u^*_{prio}| |H_f| \right) \tag{13}$$

the three-step process being re-iterated until we get a fixed point $\mathcal{M}_{opt,norm} = \mathcal{M}^{(\infty)}$.

5   A NUMERICAL ILLUSTRATION

We restrict our study to a benchmark of two-dimensional Poisson problems. We conjecture that the two following mesh adaptation methods produce L^2 convergent solutions to continuous. The first method, the Hessian-based method (with $p = 2$), is just heuristically relying on usual finite-element estimates. The second method, our novel norm-oriented method, is directly built on the minimisation of the L^2 error norm. We do not consider goal-oriented applications, for which examples of computations can be found in [11] and [2].

5.1 Numerical features

In [4], a mesh-adaptative full-multigrid (FMG) algorithm relying on the Hessian-based adaptation criterion is designed. We first describe in short this algorithm for the Hessian-based option. A sequence of numbers N_k of vertices is specified, from a coarse mesh to finer one $N_0 = N, N_1 = 4N, N_2 = 16N, N_3 = 64N, ...$ For each mesh size N_k, a sequence of adapted meshes of size N_k is built by iterating the following loop:
(1) computing a solution,
(2) computing the optimal metric,
(3) building the adapted mesh.
In (1), a multi-grid V-cycle is applied to a sufficient convergence. In (2), approximations of the Hessians are performed as in [11]. When changing of mesh, an interpolation is applied in order to enjoy a good initial condition. About 4 adaptation iterations are applied at each mesh fineness N_k.

The extension of the above loop to norm-oriented adaptation consists in replacing the single Hessian evaluation by:
- the computation of the corrector, using MG and the best available (interpolated to current mesh) previous evaluation,
- the computation of the adjoint, using MG and also the best available (interpolated to current mesh) previous evaluation,
- the evaluation of (13).

5.2 APPLICATION TO A 2D BOUNDARY LAYER

This test case is taken from [7]. We solve the Poisson problem $-\Delta u = f$ in $]0, 1[\times]0, 1[$ with Dirichlet boundary conditions and a right-hand side f chosen for having:

$$u(x, y) = [1 - e^{-\alpha x} - (1 - e^{-\alpha})x]4y(1 - y).$$

The coefficient α is chosen equal to 100. The graph of the solution is depicted in Figure 1a. In Figure 1b , we show a set of FMG calculations for the considered test case. The number of vertices of the successive meshes is supported by the horizontal axis, from 120 vertices to 30,000 vertices. The vertical axis gives the L^2-norm of the approximation error $|u - u_h|_{L^2}$ obtained on the mesh. Its variation with respect to number of vertices is compared in Figure 1b for the three following algorithms: (a) the uniform-mesh FMG, and (b) the Hessian-based adaptative FMG, and (c) the norm-oriented adaptative FMG. We observe that both adaptation methods carry an important improvement with respect to uniform-grid FMG (25921 vertices on finest mesh). For essentially the same number of vertices (32318), the Hessian option gives an error divided by 47. The norm-oriented option appears as better, with an error divided by 208 with 29485 vertices.
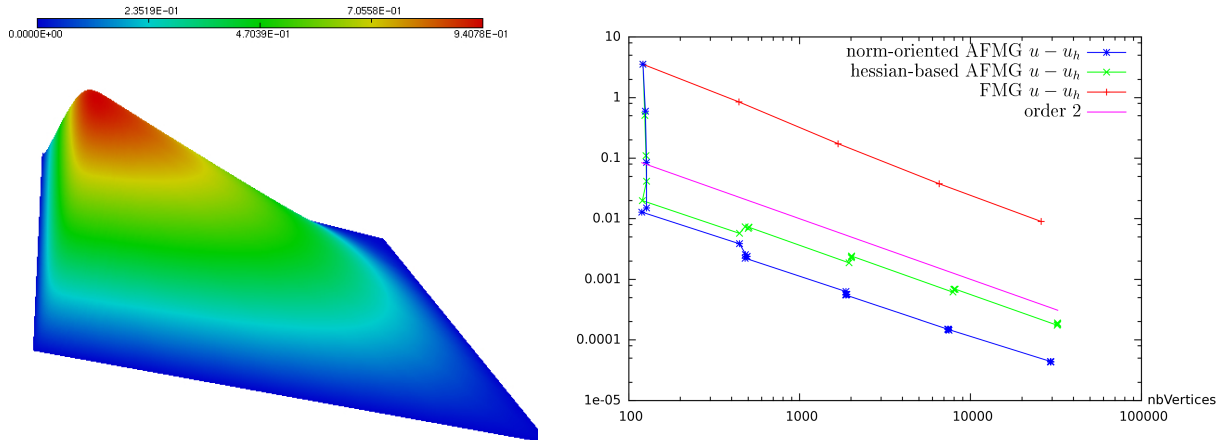
Figure 1: Fully 2D Boundary layer test case : (a) sketch of the solution, (b) convergence of the error norm $|u - u_h|_{L^2}$ as a function of number of vertices in the mesh for (+) non-adaptative FMG, (×) Hessian-based adaptative FMG, (∗) norm-oriented adaptative FMG.

6 EULER FLOW

6.1 Methods

The above method has been extended to Euler flow adaptation. Let us denote $\Psi(W) = 0$ the steady Euler equations where $W = \{\rho, \rho\mathbf{u}, \rho E\}$ is the set of conservation variables. Let $\Psi_h(W_h) = 0$ be its discretization by a vertex-centered second-order upwind scheme. The DC evaluation of the corrector writes:

$$\frac{\partial \Psi_h}{\partial W}\bar{W}'_{DC} = \frac{4}{3}R_{h/2 \to h}\Psi_{h/2}(P_{h \to h/2}W_h), \quad W'_{DC} = \bar{W}'_{DC} - (\pi_h W_h - W_h). \tag{14}$$

Then

$$\frac{\partial \Psi_h}{\partial W}g'_{DC} = W'_{DC}. \tag{15}$$

In practice, a nonlinear version of (15) is used. The rest of the algorithm is very similar to a goal-oriented algorithm, for which we follow the lines of [11].

6.2 An example

We consider the geometry provided for the 1st AIAA CFD High Lift Prediction Workshop (Configuration 1). We consider an inflow at Mach 0.2 with an angle of attack of 13 degrees. Three adaptation strategies are compared: the first one controls the interpolation error on the density, velocity and pressure in L^1 norm, the second controls the interpolation error on the Mach number while the third one is based on the norm-oriented approach and controls the norm of the approximation error $||W - Wh||_{L^2}$. For each case, five adaptations at fixed complexity are performed for a total of 15 adaptations with the following complexities: [160 000, 320 000, 640 000]. This choice leads to final meshes having around 1 million vertices. The residual for the flow solver convergence is set to 10^{-9}

for each case. The generation of the anisotropic meshes is done with the local remeshing strategy of [13]. The surface meshes and the velocity iso-lines are depicted in Figure 2. Depending on the adaptation strategy, completely different flow fields are observed. The adaptation on the Mach number reveals strong shear layers at the wing tip that are not present in the norm oriented approach. On the contrary, recirculating flows are observed on the norm oriented approach while not being observed on the Mach number adaptation. For each case, the wakes have different features. Note that the accuracy near the body is not equivalent. For the L^1 norm adaptation error and norm oriented approaches, the far-field and inflow are much more refined than in the Mach number adaptation. This leads to unresolved phenomena for the final considered complexity. This example illustrates the need to control the whole flow field. Indeed, if the adaptation on the Mach number can provide a second-order convergent field, there is no guarantee on the other fields (density, pressure, velocity,...). In addition, the adaptation with the norm-oriented approach tends to increase the refinement also at the inflow boundary condition and also at the far-field although the interpolation error (on all variables) is negligible in these areas. Consequently, it seems of main interest to control all the sources of error, especially when the final intent is to certify a flow simulation.

7 CONCLUSION

The norm-oriented mesh adaptation method is an answer to a well-formulated problem: we choose an error norm and prescribe a number of nodes and we have to find the mesh giving the smallest approximation error in that norm. The norm-oriented mesh adaptation method transforms the problem into an optimization problem which is mathematically well-posed. For this, a Defect-Correction corrector is built from a finer-mesh defect correction principle. The norm-oriented method is presented as a natural extension of the goal-oriented method which, in our formulation, is itself a natural extension of the Hessian-based method. More precisely, while the Hessian-based method solves only the EDP under study, the goal-oriented method also solves an adjoint system (with linearised operator, transposed). The norm oriented solves three systems, a corrector (linearised system with an adhoc RHS), an adjoint (linearised and transposed, with the corrector as RHS), and the EDP itself. The three algorithms have in common an anisotropic *a priori* error analysis and a metric-based mesh parametrisation. The Hessian-based method produces convergent solution fields but does not take into account the precise equation and discretization. The goal-oriented method takes into account equation and discretization, but is too focused on a particular output and does not produce convergent solution fields. The norm-oriented method has the advantages of both. For elliptic problems, the Hessian-based approach is nearly optimal as suggested by finite-element estimates. However the presented comparisons seem to indicate that the novel method carries a good improvement. We have also proposed a preliminary application to an inviscid compressible flow. New computations will be shown during the conference.
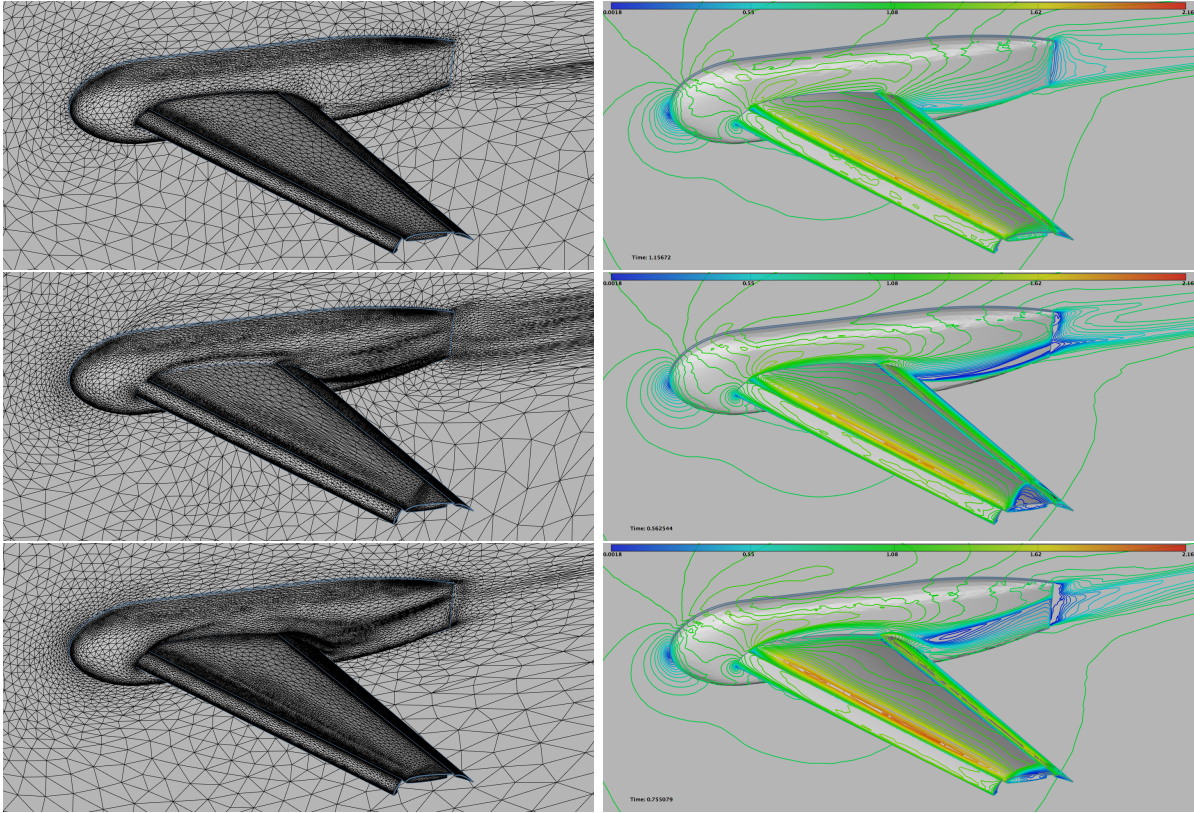
Figure 2: Surface mesh and velocity iso-values when controlling the sum of the L^1 norm of the interpolation error on the density, velocity and pressure (top), the Mach number (middle) and the norm $||W - Wh||_{L^2}$ with the norm oriented approach (bottom).

8   ACKNOWLEDGEMENTS

REFERENCES

[1] A. Belme. *Aérodynamique instationnaire et méthode adjointe.* PhD thesis, Université de Nice Sophia Antipolis, Sophia Antipolis, France, 2011. (in French).

[2] A. Belme, A. Dervieux, and F. Alauzet. Time accurate anisotropic goal-oriented mesh adaptation for unsteady flows. *J. Comp. Phys.*, 231(19):6323–6348, 2012.

[3] M. Berger. *A panoramic view of Riemannian geometry.* Springer Verlag, Berlin, 2003.

[4] G. Brèthes, O. Allain, and A. Dervieux. A mesh-adaptive metric-based Full-Multigrid for the Poisson problem. *submitted to I.J. Numer. Meth. Fluids*, 2014.

[5] M.J. Castro-Díaz, F. Hecht, B. Mohammadi, and O. Pironneau. Anisotropic unstructured mesh adaptation for flow simulations. *Int. J. Numer. Meth. Fluids*, 25:475–491, 1997.

[6] J. Dompierre, M.G. Vallet, M. Fortin, Y. Bourgault, and W.G. Habashi. Anisotropic mesh adaptation: towards a solver and user independent CFD. In *AIAA 35th Aerospace Sciences Meeting and Exhibit*, AIAA-1997-0861, Reno, NV, USA, Jan 1997.

[7] L. Formaggia and S. Perotto. Anisotropic a priori error estimates for elliptic problems. *Numer. Math.*, 94:67–92, 2003.

[8] A. Loseille. *Adaptation de maillage anisotrope 3D multi-échelles et ciblée à une fonctionnelle pour la mécanique des fluides. Application à la prédiction haute-fidélité du bang sonique.* PhD thesis, Université Pierre et Marie Curie, Paris VI, Paris, France, 2008. (in French).

[9] A. Loseille and F. Alauzet. Continuous mesh framework. Part I: well-posed continuous interpolation error. *SIAM Journal on Numerical Analysis*, 49(1):38–60, 2011.

[10] A. Loseille and F. Alauzet. Continuous mesh framework. Part II: validations and applications. *SIAM Journal on Numerical Analysis*, 49(1):61–86, 2011.

[11] A. Loseille, A. Dervieux, and F. Alauzet. Fully anisotropic goal-oriented mesh adaptation for 3D steady Euler equations. *J. Comp. Phys.*, 229:2866–2897, 2010.

[12] A. Loseille, A. Dervieux, P.J. Frey, and F. Alauzet. Achievement of global second-order mesh convergence for discontinuous flows with adapted unstructured meshes. In *37th AIAA Fluid Dynamics Conference and Exhibit*, AIAA-2007-4186, Miami, FL, USA, Jun 2007.

[13] A. Loseille and V. Menier. Serial and parallel mesh modification through a unique cavity-based primitive. In J. Sarrate and M. Staten, editors, *Proceedings of the 22th International Meshing Roundtable*, pages 541–558. Springer, 2013.

[14] F. Magoules. *Computational Fluid Dynamics*. CRC Press, Boca Raton, London, New York, Washington D.C., 2011.